Eur. Phys. J. C (2008) 56: 467–477
DOI 10.1140/epjc/s10052-008-0675-6

THE EUROPEAN PHYSICAL JOURNAL C

Regular Article - Theoretical Physics

One-loop $gg \to b\bar{b}$ effects in the main irreducible background to exclusive $H \to b\bar{b}$ production at the LHC

A.G. Shuvaev[1], **V.A. Khoze**[1,2,a], **A.D. Martin**[2], **M.G. Ryskin**[1,2]

[1]Petersburg Nuclear Physics Institute, Gatchina, St. Petersburg 188300, Russia
[2]Department of Physics and Institute for Particle Physics Phenomenology, Durham University, Durham DH1 3LE, UK

Received: 12 June 2008 / Published online: 31 July 2008

Abstract We calculate the amplitude of $gg \to b\bar{b}$ production for the colour singlet, $J_z = 0$, di-gluon state at $\mathcal{O}(\alpha_S^2)$ order. We consider the cancellation and a realistic cut-off, of the infrared divergent terms. We show that the one-loop radiative QCD contributions effectively *reduce* the Born level result for the central exclusive $b\bar{b}$ cross section at the LHC. This process is essentially the only irreducible QCD background to the exclusive $H \to b\bar{b}$ signal.

1 Introduction

The search for and identification of the Higgs boson(s) are two of the main goals of the LHC. Once the Higgs boson is discovered, it will be of primary interest to determine its spin and parity, and to measure precisely its mass and couplings, in particular the $Hb\bar{b}$ Yukawa coupling. An important contribution to the comprehensive study of the Higgs sector can be provided by central exclusive diffractive (CED) Higgs boson production,

$$pp \to p \oplus H \oplus p, \tag{1}$$

where the $\oplus$ signs denote the presence of the large rapidity gaps (LRG); see, for example [1–6]. The process is sketched in Fig. 1. In such an exclusive process there is no hadronic activity between the outgoing protons and the decay products of the central (Higgs) system. The $b\bar{b}$ decay mode of the Higgs is especially attractive, since its observation would allow for a detailed study of the MSSM Higgs sector [7–9]. Indeed, for certain BSM scenarios, it may become *the* Higgs discovery channel [7, 10]. The experimental study of central exclusive Higgs production is one of the key theoretical motivations behind the FP420 project [11, 12], which proposes to complement the CMS and ATLAS experiments at the LHC by installing additional forward proton detectors 420 m away from the interaction region.

To avoid the production of new secondaries across the LRG, the colour flow caused by the active gluons (which participate in $gg \to H$ fusion) must be screened by another, softer, gluon, see Fig. 1. Thus, in the exclusive process the central system (the Higgs boson) is actually generated by a specific $gg^{\rm PP}$ gluon state, where the PP superscript is to indicate that each hard (active) gluon comes from colour singlet t-channel (pomeron) exchange. Moreover, the presence of the second t-channel screening gluon leads to an additional loop integration. The integration over the transverse momentum in this loop results in a $J_z = 0$, CP-even selection rule [13, 14]. Here J_z is the projection of the total angular momentum along the beam axis of the proton.

The $J_z = 0$ selection rule is one of the major reasons why central exclusive production is so attractive for Higgs studies. First, it readily permits a clean determination of the quantum numbers of the observed new resonance, which will be dominantly produced in a scalar state. A second direct consequence of this rule is the unique opportunity to study directly the $Hb\bar{b}$ Yukawa coupling of the Higgs-like

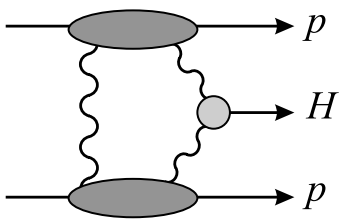

Fig. 1 The mechanism for central exclusive Higgs production, $pp \to p \oplus H \oplus p$. The Higgs boson is produced by the fusion of two so-called active gluons. The screening gluon on the left is required to ensure a colour neutral system across the rapidity gaps. We do not show the additional screening corrections which must be included to ensure the survival of the rapidity gaps from population from secondaries resulting from soft rescattering

[a] e-mail: v.a.khoze@durham.ac.uk

bosons in central exclusive processes. The potentially copious b jet (QCD) background is controlled by a combination of the $J_z = 0$ selection rule [13, 14] (which strongly suppresses the leading-order QCD $b\bar{b}$ production), the colour and spin factors and, finally, the excellent resolution of the missing mass to the measured outgoing protons.[1] It is the possibility to observe directly the dominant $b\bar{b}$ decay mode of the SM Higgs with $M_H \lesssim 140$ GeV that first attracted attention to exclusive production at the LHC. As is well known, the direct determination of the $Hb\bar{b}$ coupling appears to be very difficult for other search channels at the LHC.

We emphasize that for forward going protons at the LHC the Higgs signal is produced by gluons in a $J_z = 0$ state whereas the LO QCD backgrounds are primarily initiated by initial states with $|J_z| = 2$. The $J_z = 0$ background contribution is suppressed for large angles by a factor m_b^2/E_{T}^2, where E_{T} is the transverse energy of the b and $\bar{b}$ jets; see for example [15, 16]. As discussed in [16, 17], the physical origin of this suppression is related to the symmetry properties of the Born helicity amplitudes $M_{\lambda_1,\lambda_2}^{\lambda_q,\lambda_{\bar{q}}}$ describing the binary background process

$$g(\lambda_1, p_A) + g(\lambda_2, p_B) \to q(\lambda_q, p_1) + \overline{q}(\lambda_{\bar{q}}, p_2). \tag{2}$$

Here, the λ_i label the helicities of the incoming gluons, and λ_q and $\lambda_{\bar{q}}$ are the (doubled) helicities of the produced quark and antiquark. The p denote the particle four-momenta ($p_{\mathrm{A}}^2 = p_{\mathrm{B}}^2 = 0$ and $p_{1,2}^2 = m^2$), with $p_{\mathrm{A}} + p_{\mathrm{B}} = p_1 + p_2$ and $s = (p_{\mathrm{A}} + p_{\mathrm{B}})^2$. It was shown in [15] that for a colour singlet, $J_z = 0$, initial state ($\lambda_1 = \lambda_2 \equiv \lambda$) the Born quark-helicity-conserving (QHC) amplitude with $\lambda_{\bar{q}} = -\lambda_q$ vanishes[2]

$$M_{\lambda,\lambda}^{\lambda_q,-\lambda_q} = 0. \tag{3}$$

For the quark-helicity-non-conserving (QHNC) amplitude for large angle production we have

$$M_{\lambda,\lambda}^{\lambda_q,\lambda_q} \sim \mathcal{O}\left(\frac{m_q}{\sqrt{s}}\right) M_{\lambda,-\lambda}^{\lambda_q,-\lambda_q}, \tag{4}$$

where the amplitude on the right-handside displays the dominant helicity configuration of the LO background process.

The main sources of background to the exclusive $H \to b\bar{b}$ production at the LHC were discussed in detail in [3, 8, 16, 21]. It was shown that all backgrounds are strongly suppressed and controllable and, in principle, can be further reduced by the appropriate optimized cuts on the final state particle configurations in such a way that the signal-to-background ratio S/B is of order 1 (or maybe even better for the MSSM Higgs case [7–9]).

Among all the QCD backgrounds, the m_b^2/E_{T}^2-suppressed di-jet $b\bar{b}$ production is especially critical, since it is practically the only one irreducible background source which cannot be decreased, either by improving the hardware (as in the case when the prolific $gg^{\mathrm{PP}} \to gg$ subprocess mimics $b\bar{b}$ production, and the outgoing gluons are misidentified as b and $\bar{b}$ jets [3]) or, for example, by cuts on the three-jet event topology (as in the case of large angle gluon radiation in the process $gg(J_z = 0) \to q\bar{q}g$, discussed in [16]). Therefore, the precise calculation of the QHNC background contribution becomes of primary importance for quantifying the signal-to-background ratio, and the accurate evaluation of the statistical significance of the $H \to b\bar{b}$ signal. In [3, 8] it was estimated that the contribution from this source was $B/S \sim 0.4$, when the Born formula for the binary cross section was used. The same LO result for the background subprocess was used for the evaluation of a statistical significance of the MSSM Higgs boson signal in [8, 9]. However, it is known [15, 16] that higher-order QCD effects may strongly affect the LO result.

First, there is a reduction coming from the self-energy insertions in the b-quark propagator, that is, from running of the b-quark mass from $\overline{m}_b(\overline{m}_b)$ to its value $\overline{m}_b(M_H) < \overline{m}_b(\overline{m}_b)$, at the Higgs scale. Here $\overline{m}_b(\mu)$ is the running b-quark mass in the $\overline{\mathrm{MS}}$ scheme [22]. Secondly, in our case, where $m_b \ll M_H$, double-logarithmic corrections of the form $(\alpha_{\mathrm{S}}/\pi)\ln^2(M_H/m_b)$ are potentially very important. These are related to the so-called non-Sudakov form factor, F_q, in the cross section which arises from the virtual diagrams with gluon exchange [15, 23–27].

For the case of the $\gamma\gamma(J_z = 0) \to b\bar{b}$ process the complete one-loop result was first calculated in [23]. For the photon–photon reaction, the double-logarithmic (DL) asymptotics for F_q has the form

$$F_q(L_m) = \sum_n c_n \left(\frac{\alpha_{\mathrm{S}}}{\pi} L_m^2\right)^n, \tag{5}$$

with $L_m \equiv \ln(M_H/m_b)$, $c_0 = 1$ and $c_1 = -8$ [15, 23]. The second (negative) term in (5) is anomalously large and dominates the Born term for $M_H > 100$ GeV. Clearly, this dominance undermines the results of any analysis based on the Born approximation.[3] The physical origin of this

[1] Current studies [11] show that the missing-mass resolution σ will be of the order of 1% for a 140 GeV Higgs boson assuming that both protons are detected at 420 m from the interaction point. The equality of the accurate missing-mass measurement of M_H with its mass determined from its decay products allows the background to be considerably suppressed.

[2] It is worth noting that in the massless limit (3) holds for any colour state of initial gluons. This is a consequence of the general property that the non-zero massless tree-level amplitudes should contain at least two positive or two negative helicity states; see for example [18, 19]. It is an example of the more general maximally-helicity-violating amplitude (MHV) rule, reviewed for example in [20].

[3] For gg^{PP} fusion, rather than $\gamma\gamma$ fusion, we might, a priori, anticipate that colour factors could make the coefficient c_1 even larger.

non-Sudakov form factor was elucidated in [15], where the explicit DL calculation at the two-loop level was performed. It was also shown that the two-loop calculation should be sufficient for a reliable evaluation of the DL effects. This was confirmed by a more comprehensive all-order study [24–27].

Recall that in the photon–photon case, the two-loop expression for the F_q is [15]

$$F_q(L_m) = (1-3\mathcal{F})^2 + \frac{\mathcal{F}^2}{3}\left(1+\frac{C_A}{C_F}\right), \tag{6}$$

with

$$\mathcal{F} = \frac{\alpha_S}{\pi} C_F L_m^2, \tag{7}$$

where $C_F = (N_c^2-1)/2N_c$, $C_A = N_c$ and $N_c = 3$ is the number of colours. The non-Sudakov logarithms come from kinematical regions where one of the *quark* propagators is soft. As is well known, there are other DL effects (the well known Sudakov logarithms [28]), which arise from virtual soft *gluon* exchange. As discussed in [15], in the case of quasi-two-jet configurations, the Sudakov and non-Sudakov effects can be factorized to good accuracy, since they correspond to very different virtualities of the internal quark and gluon lines. For final state radiation, the Sudakov effects can be implemented in parton shower Monte Carlo models in the standard way. For the gg^{PP} initial state, the Sudakov factors are explicitly incorporated in the unintegrated gluon densities [1, 2].

Unfortunately, from a phenomenological perspective, it is dangerous to rely on the DL results, since experience shows that formally subleading (SL) corrections may be numerically important. That is why an accurate evaluation of the QCD $b\bar{b}$ background to the central exclusive process

$$pp \to p \oplus (H \to b\bar{b}) \oplus p \tag{8}$$

requires, first of all, the calculation of the exact one-loop correction to the Born $gg^{PP} \to b\bar{b}$ amplitude; that is, to the hard subprocess $gg \to b\bar{b}$ in a colour singlet, $J_z = 0$, initial state.

The calculation is described in Sect. 2, where the result is presented as the sum of standard integrals corresponding to the box, triangle and self-energy Feynman diagrams with the scalar propagators. In Sect. 3 the infrared divergencies of the virtual loop amplitude are discussed. These divergences are canceled either by real gluon emission or by the diagrams where an additional virtual gluon is emitted off the second t-channel (screening) gluon in the whole $pp \to p \oplus b\bar{b} \oplus p$ amplitude. Numerical estimates are mentioned as an illustration in Sect. 4.

2 Calculation of the $gg \to b\bar{b}$ amplitude

We consider the amplitude defined by

$$T_{gg\to b\bar{b}} = \sum_{a,b}\sum_{\epsilon_1,\epsilon_2} M_{ab}^{\epsilon_1,\epsilon_2}\delta_{ab}\delta_{\epsilon_1\epsilon_2}, \tag{9}$$

where a and b are the colour indices ($a, b = 1, 2, \ldots, N_c^2-1$), and the $\epsilon_{1,2}$ are the transverse polarization vectors of the incoming gluons. Introducing the outgoing quark spinors, the amplitude can be written as

$$T_{gg\to b\bar{b}} = \bar{u}(p_1)T(\not{p})v(p_2), \tag{10}$$

where the matrix T is built from the four-momenta p involved in the reaction, $\not{p} \equiv p_\mu\gamma^\mu$. There are three independent four-momenta, which we take to be p_1, p_2 of b and $\bar{b}$, and the difference of the incoming gluon momenta, $p_A - p_B$. The matrix $\not{p}_1$ can be moved to the left, and $\not{p}_2$ to the right, until they disappear upon acting on the spinor,

$$\bar{u}(p_1)\not{p}_1 = m\bar{u}(p_1), \qquad \not{p}_2 v(p_2) = -mv(p_2), \tag{11}$$

where $m \equiv m_b$. This rearrangement reduces the amplitude to two spinor structures, corresponding to the following helicity-violating and helicity-conserving terms:[4]

$$T_{gg\to b\bar{b}} = \bar{u}(p_1)v(p_2)T_1 + \bar{u}(p_1)(\not{p}_A - \not{p}_B)v(p_2)T_2. \tag{12}$$

The scalar coefficients $T_{1,2}$ depend on the invariants

$$s = (p_1+p_2)^2, \qquad t = (p_A-p_1)^2, \qquad u = (p_A-p_2)^2. \tag{13}$$

The function T_1 is symmetric with respect to t–u interchange, while T_2 is antisymmetric. Their calculation requires an evaluation of the spinor traces, which can easily be carried out with the help of an analytical program.

2.1 The Born contribution

As discussed above, only the helicity-violating piece contributes at the Born level to the $J_z = 0$ amplitude, that is, the sum $(++) + (--)$ of the helicities of the incoming gluons,

$$T_1^{Born} = 4\pi\alpha_S C_F 2m\left[\frac{1}{m^2-t} + \frac{1}{m^2-u}\right], \qquad T_2^{Born} = 0. \tag{14}$$

[4] In principle, there are two other possible structures related to the fourth vector $e_\mu \sim \varepsilon_{\mu\nu\lambda\sigma}p_1^\nu(p_A-p_B)^\lambda p_2^\sigma$ namely, $u(p_1)\gamma^5 v(p_2)$ and $\bar{u}(p_1)(\not{p}_A - \not{p}_B)\gamma^5 v(p_2)$, but they do not appear for our subprocess.

2.2 One-loop effects

In order to evaluate the one-loop effects, the loop integrations are reduced to master scalar integrals, which we denote by I. The final result is written in terms of the set of these integrals. The Feynman gauge is used in the $\overline{\rm MS}$ scheme with the dimensional parameter of the order of the characteristic virtualities of the process, $4\pi\mu^2 = -k^2 = s/4$. The ultraviolet (UV) divergencies are renormalized, to first order in $\alpha_{\rm S}$, by the gluon and quark Z-factors, mass and charge renormalization in the Born term.

For central exclusive production, the effective luminosity of the incoming active gluons,

$$\frac{M^2\partial\mathcal{L}(gg^{\rm PP})}{\partial y\partial M^2} = \hat{S}^2 L^{\rm excl}, \tag{15}$$

is given by the integral expression [2]

$$L^{\rm excl} = \left(\frac{\pi}{(N_c^2-1)b}\int \frac{{\rm d}Q_t^2}{Q_t^4} f_g\big(x_1^+, x_1'^+, Q_t^2, \mu^2\big) \times f_g\big(x_2^-, x_2'^-, Q_t^2, \mu^2\big)\right)^2, \tag{16}$$

where the integration is over the transverse momentum of the gluon loop in Fig. 1. Here b is the t-slope, corresponding to the momentum transfer distributions of the colliding protons, and $x_{1,2}$ are the light-cone momentum fractions carried by the active gluons.[5] The colour flow due to the active gluons is screened by the second t-channel gluon, which carries the momentum fractions $x_1'^+$ and $x_2'^-$. The gap survival factor $\hat{S}^2$ accounts for the soft rescattering effect. Thus, $\hat{S}^2$ is the probability that the rapidity gaps are not populated by secondaries produced in possible soft rescattering [1, 2, 29, 30]. The integral over the gluon transverse momentum Q_t is convergent, in both the ultraviolet and infrared regions. The contribution of the low Q_t domain is suppressed by Sudakov-like form factors incorporated in the unintegrated gluon densities f_g.

Due to the presence of the second t-channel (screening) gluon, there is no infrared divergency in the matrix element of the "hard" $gg(J_z = 0) \to b\bar{b}$ subprocess. This opens up the possibility to regularize the infrared (IR) divergences by a fictitious gluon mass m_g. In order to preserve gauge invariance, the mass m_g can be formally introduced via the Higgs mechanism.[6] Of course, this will generate additional diagrams with Higgs boson exchange or production. Such Higgs boson exchange will provide 'cross-talk' between the 'hard' matrix element and the second t-channel (screening) gluon. As a result, we set $m_g = Q_t$; that is, we introduce a physical infrared cut-off in the exclusive $b\bar{b}$ production. After this, the contribution of the "artificial" Higgs boson diagrams can be eliminated by choosing the mass of the "Higgs" boson to be very large, $M_H^2 \gg s$. Since there is no need to regularize the integral (16), here we will work in the $D = 4$ world, so the polarizations of our gluons are constrained to $D = 4$ space.

The structures $T_{1,2}$ in (12) both can contribute to the one-loop correction. We begin with the helicity-conserving part

$$T_2(s,t,u) = A_2(s,t,u) - A_2(s,u,t).$$

We retain only the quark mass $m = 0$ contribution. The function $A_2(s,t,u)$ is given by the set of Feynman diagrams shown in Fig. 2. The second term in the expression for $T_2(s,t,u)$ takes care of $t \leftrightarrow u$ interchange. When performed naively, a straightforward calculation results in a complete cancellation between the two terms. So we have $T_2(s,t,u) = 0$ at the one-loop level, similar to the Born term.[7]

The QHNC part of the amplitude is given by two terms:

$$T_1(s,t,u) = A_1(s,t,u) + A_1(s,u,t), \tag{17}$$

where the second term, as in the previous case, comes from u-channel crossing. Recall that the amplitude T_1 is symmetric with respect to t–u interchange. The function $A_1(s,t,u)$ is calculated from the same set of Feynman diagrams as is shown in Fig. 2. As in the Born term, the one-loop amplitude vanishes if we set $m = 0$. Here we present an expression for the amplitude to lowest order in mass; that is

$$A_1 = 4\pi\alpha_{\rm S}\frac{\alpha_{\rm S}}{4\pi} m\big[A_0 + A_q + A_g + A_{qg}\big], \tag{18}$$

where m is the quark pole mass, $m = \overline{m}_b(\overline{m}_b)$, and the running coupling constant is taken at the scale μ, with $\alpha_{\rm S} = \alpha_{\rm S}(\mu^2)$. The function A_0 is made up of pieces coming from

[5] The superscript $+$ $(-)$ is to indicate the light-cone momentum fraction of the momentum q_1, (q_2) of the first (second) colliding proton; that is, $Q_\mu = x_1'^+ q_{1\mu} + x_2'^- q_{2\mu} + Q_{t\mu}$.

[6] This way of introducing the infrared cut-off m_g was used, for example, in the original BFKL calculations [31, 32].

[7] At first sight, it appears that the zero value of T_2 is in contradiction with [33–35], which leads to a non-zero result for the one-loop (cut-non-reconstructible) QHC amplitude $gg(J_z = 0) \to b\bar{b}$ in dimensional regularization, assuming that the incoming gluons are on-mass-shell. This non-zero cut-non-reconstructible contribution comes from a ratio of the form $\epsilon/\epsilon = {\rm const}$, where the denominator (that is, the factor $1/\epsilon$) is of infrared origin. However, in our case, due to the presence of the screening gluon, the (transverse) size of the interaction region is limited by a value of order of $\sim 1/Q_t$. This generates a dynamical infrared cut-off at a scale $\sim Q_t^2$, which, in our calculation, is taken care of by introducing an effective gluon mass $m_g = Q_t$. As a result, the infrared singularities are absorbed in the unintegrated gluon structure functions. The factor $1/\epsilon$ is replaced by $\ln(\mu/m_g)$, and as $\epsilon \to 0$ we obtain $T_2 = 0$. Thus our procedure is quite different from the on-mass-shell calculations.

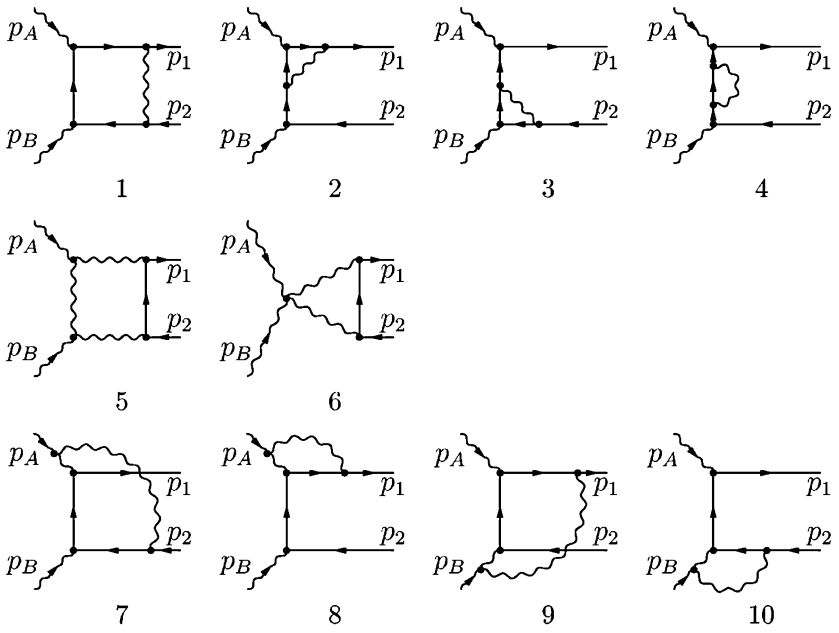

Fig. 2 One-loop diagrams contributing to the $gg \to b\bar{b}$ process

the logarithmically divergent scalar master integrals with two propagators. The $1/\epsilon$ terms, appearing in dimensional regularization, are subtracted by the counterterms coming from the field Z-factors, quark mass and coupling constant renormalization in the Born term. To be precise, A_0 collects what is not included in the master scalar integrals I that are given in Appendix A. In fact, A_0 depends on which form has been assumed for the gluon polarizations in dimensional regularization. That is, it is a matter of whether the transverse tensor lies exactly in two-dimensional space $D-2=2$, or whether it has an admixture of the extra dimension, $D-2=2+2\epsilon$. As we discussed, in central diffractive production the active incoming gluons are screened (in the whole amplitude of the *exclusive* process) by a second t-channel gluon; see Fig. 1. In this external loop we have neither infrared nor UV divergencies. Thus the polarizations of incoming gluons lie in two-dimensional $D-2=2$ space. Moreover, when using the unintegrated gluons obtained via the KMR prescription [36, 37], from the integrated $\overline{\rm MS}$ gluon given by the global parton analyses, we have to account for the fact that the whole gluon renormalization factor Z_3 is already included in the incoming parton distribution. So the matrix element of the 'hard' subprocess must be calculated with the Z-factors equal to 1 for all 'external' lines (just as is the case when the external lines are on-mass-shell). In other words, here we present the result of the calculation[8] with $Z_3 = Z_2 = 1$.

[8]The renormalization factor, Z_2, of the b-quark is included in the evolution which describes the fragmentation of the b-quark jet.

The result obtained for $Z_2 = 1$ and $Z_3 = 1$, with the infinite parts subtracted, has the form

$$A_0^{D-2=2} = \frac{1}{t}\Bigg[-4C_{\rm F}N_{\rm c}\ln\frac{m^2}{m_g^2} + C_{\rm F}\frac{5N_{\rm c}^2-1}{N_{\rm c}}\ln\frac{m^2}{4\pi\mu^2} - 24C_{\rm F}^2\Bigg]. \tag{19}$$

The other functions in (18) are given by the finite parts of the individual Feynman diagrams shown in Fig. 2 with the colour coefficients c_i,

$$c_1 = c_4 = C_{\rm F}^2 = \left[\frac{N_{\rm c}^2-1}{2N_{\rm c}}\right]^2,$$

$$c_2 = c_3 = -\frac{1}{2N_{\rm c}}C_{\rm F} = -\frac{1}{2N_{\rm c}}\frac{N_{\rm c}^2-1}{2N_{\rm c}},$$

$$c_5 = N_{\rm c}C_{\rm F} = N_{\rm c}\frac{N_{\rm c}^2-1}{2N_{\rm c}},$$

$$c_6 = N_{\rm c}^2-1,$$

$$c_7 = c_9 = -\frac{1}{2}N_{\rm c}C_{\rm F} = -\frac{1}{2}N_{\rm c}\frac{N_{\rm c}^2-1}{2N_{\rm c}},$$

$$c_8 = c_{10} = -\frac{1}{2}N_{\rm c}C_{\rm F} = -\frac{1}{2}N_{\rm c}\frac{N_{\rm c}^2-1}{2N_{\rm c}}.$$

The master integrals, $I^q_{0000}(s,t)$ etc., appearing in the expressions below, are given in Appendix A. We have

$$A_q = 4c_1 I^q_{0000}(s,t)s + I^q_{0101}(t)\frac{2[(2s+t)(c_2+c_3)+2(2s-t)c_1-2c_4 s]}{st},$$

$$
\begin{aligned}
A_g &= 4I^g_{0000}(s,t)c_5 s + 3I^g_{1000}(s)[c_6-2c_5] - 4c_5 I^g_{0100}(t)\\
&\quad + I^g_{1010}(s)\frac{4[-(3s+2t)c_5+c_6 s]}{s^2}\\
&\quad + I^g_{0101}(t)\frac{4(2s+t)c_5}{st},\\
A_{qg} &= I^{qg}_{0000}(u,t)\frac{-[2s^2+3st+3t^2](c_7+c_9)}{s}\\
&\quad + I^{qg}_{1000}(u)\frac{3(s+t)(c_7+c_9)}{s}\\
&\quad + I^{qg}_{1000}(t)\frac{-3(c_7+c_9)t}{s}\\
&\quad + I^{qg}_{0010}(u)\frac{(c_7+c_9)(2s+3t)}{s}\\
&\quad - I^{qg}_{0010}(t)\frac{(c_7+c_9)(s+3t)+2(c_8+c_{10})s}{s}\\
&\quad + I^{qg}_{1010}(u)\frac{-4(c_7+c_9)}{s+t}\\
&\quad + 2I^{qg}_{1010}(t)\frac{(c_8+c_{10})(t-2s)+2(c_7+c_9)s}{st}.
\end{aligned}
$$

3 The infrared contribution

The amplitude T_1 contains logarithmic infrared (IR) divergences which in the formulae presented above are regularized by the effective gluon mass m_g cut-off. These IR divergent terms are essentially the usual Sudakov form factors; that is, the probability not to emit additional gluons in the *exclusive* process $pp \to p \oplus b\bar{b} \oplus p$.

The Sudakov-like form factor, due to emission from the initial active gluons, is equal to

$$
S(Q_t,\mu) = \exp\left(-\int_{Q_t^2}^{\mu^2}\frac{\alpha_S}{2\pi}\frac{dk_t^2}{k_t^2}\int_0^{1-\Delta} z P_{gg}(z)\,dz\right), \quad (20)
$$

with $P_{gg}(z)$ being the gluon–gluon Altarelli–Parisi LO splitting function corresponding to real gluon emission, and $\Delta = k_t/(\mu+k_t)$. It was already included in the effective gluon–gluon luminosity $\mathcal{L}(gg^{\rm PP})$ used to calculate the exclusive cross section [2]. Therefore, we have to subtract the term

$$
T_1^{\rm Born}\left(-\int_{Q_t^2}^{\mu^2}\frac{\alpha_S}{2\pi}\frac{dk_t^2}{k_t^2}\int_0^{1-\Delta} z P_{gg}(z)\,dz\right) \quad (21)
$$

from the amplitude T.

As discussed above, because of the presence of a screening gluon, the infrared cut-off is given by the transverse momentum (virtuality) of the incoming active gluon, and in the expressions for the amplitudes A_g and A_{qg}, where the 'internal' gluon is radiated from a gluon line, we replace m_g by Q_t. This cancels the main ($\propto \ln^2(m_g^2)$) part of the IR divergency

$$
T_1 \simeq 2m(4\pi\alpha_S)N_c C_F\frac{\alpha_S}{\pi}\left(\frac{1}{t}+\frac{1}{u}\right)\ln^2\left(s/m_g^2\right). \quad (22)
$$

The logarithmic IR divergency in the amplitude A_q is canceled after accounting for the real soft gluon emission in the b-quark jet. Usually, in Monte Carlo simulations and/or jet searching algorithms, such emission is described by LO quark evolution. So we have to subtract the term

$$
T_1^{\rm Born}\left(-\int_{k_{t0}^2}^{\mu^2}\frac{\alpha_S}{2\pi}\frac{dk_t^2}{k_t^2}\int_0^{1-\Delta_q} P_{qq}(z)\,dz\right), \quad (23)
$$

where now $P_{qq}(z)$ is the quark–quark splitting function; the lower limit k_{t0} is fixed by the experimental conditions – gluons with transverse momenta with respect to the b jet axis that have $k_t < k_{t0}$ are included in the definition of the jet. The kinematic limit is $\Delta_q = 2k_{t0}/\sqrt{s}$. As a result, we put $m_g = k_{t0}$ in the expression[9] for A_q.

4 The double-logarithmic contributions

As was discussed in the Introduction, large double-logarithmic terms can be of Sudakov or non-Sudakov origin. The Sudakov contributions reflect the possibility to emit additional soft gluons. They are absorbed (and subtracted) in the definitions of the $gg^{\rm PP}$ luminosity and in the prescription for the quark jet search. The non-Sudakov logarithms come from the kinematical domain in which one of the quark propagators in the diagram is soft. In the case of the $\gamma\gamma \to b\bar{b}$ process, this contribution was numerically quite large,

$$
T_1^{\text{non-Sud}}(\gamma\gamma\to b\bar{b}) \simeq T_1^{\rm Born}\cdot 3C_F\frac{\alpha_S}{4\pi}\ln^2\left(s/m_b^2\right); \quad (24)
$$

see (5). In our case, with a larger number of diagrams and larger colour coefficients in the one-loop $gg \to b\bar{b}$ Feynman graphs, there is a danger that we could find an even larger non-Sudakov DL correction. However, the situation appears to be different. Contributions which correspond to diagrams with three gluons in the loop and to diagrams with two gluons have different signs. This is analogous to the destructive

[9] There still remains a contribution proportional to the first power of $\ln(m_g)$, which is not canceled by the subtractions (21) and (23). This contribution arises from large angle soft gluon emission, when we cannot neglect the interference between the emission from the gluon and from the quark lines. Such interference, hidden in the amplitude A_{qg}, is not included, either in the definition of the jet or in the effective $gg^{\rm PP}$ luminosity. The corresponding IR divergency is cut off by the presence of the screening gluon in the effective $gg^{\rm PP}$ luminosity; that is by the gluon transverse momentum Q_t; to mimic this fact we set $m_g = Q_t$, as before.

interference between the emission of a photon from the incoming and the outgoing electron for small angle scattering. Unlike the $\gamma\gamma \to b\bar{b}$ case, here we have additional double-logarithm contributions coming from A_g and A_{qg}, such that the final result does not contain a large numerical coefficient

$$T_1^{\text{non-Sud}}(gg \to b\bar{b}) \simeq T_1^{\text{Born}} \cdot (3C_F - N_c)\frac{\alpha_S}{4\pi}\ln^2(s/m_b^2). \tag{25}$$

We see that, instead of the naively expected factor $3N_c$ (which indeed comes from the first term of A_g; that is, from the integral I^g_{0000}), the coefficient in the sum of the A_g and A_{qg} amplitudes in front of the non-Sudakov double-logarithm is proportional to $3N_c - 4N_c = -N_c$.

5 Discussion

To evaluate the role of the one-loop correction numerically, we first calculate the cross section:

$$\frac{d\sigma^{(0)+(1)}}{d\cos\theta} = \frac{1}{32\pi s}\left(\frac{1}{2(N_c^2-1)}\left(T_1^{\text{Born}} + T_1\right)\right)^2, \tag{26}$$

which must be multiplied by the effective gluon–gluon luminosity (15) [2]. The results are shown in Fig. 3 for different values of the infrared cut-offs Q_t and k_{t0}. The scale is taken to be $4\pi\mu^2 = s/4$.

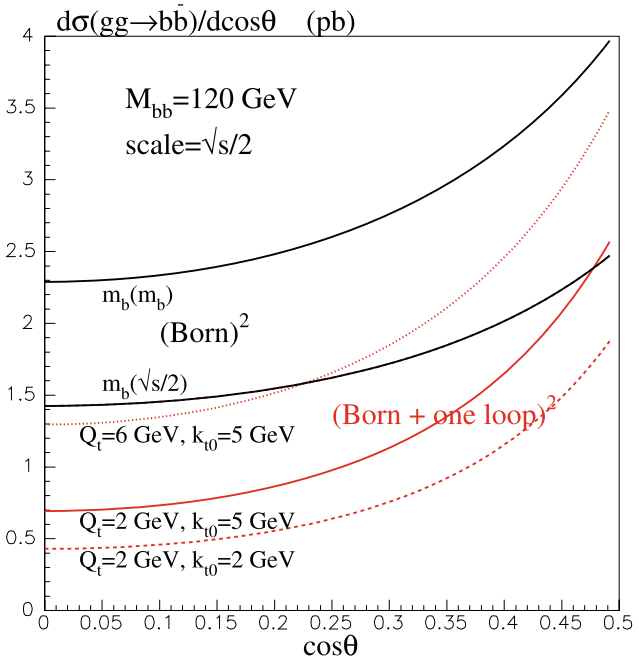

Fig. 3 Angular dependence of the exclusive one-loop $b\bar{b}$ cross section for different choices of the infrared cut-offs; the values of the cut-offs are given under the corresponding curves. For comparison, we also show, by the two upper solid curves, the Born results for two choices of the running b-quark mass

The value $Q_t = 2$ GeV corresponds to the maximum of the integrand in (16) for the exclusive production of a Higgs boson of mass $M_H = 120$ GeV at the LHC. The choice $k_{t0} = 5$ GeV appears to be reasonable for the standard b-quark jet searching; the gluons with transverse momentum (with respect to the b jet axis) of $k_t > 5$ GeV can be considered as separate jets. To demonstrate the dependence of the cross section $\sigma^{(0)+(1)}$ on the values of Q_t and k_{t0}, we also show the predictions for $Q_t = 6$ GeV and $k_{t0} = 2$ GeV. We use a b-quark pole mass $\overline{m}_b(\overline{m}_b) = 4.2$ GeV and take $\alpha_S(M_Z) = 0.118$. For lower infrared cut-offs the probability not to emit an additional gluon decreases, and the cross section is smaller.

For comparison, we also show in Fig. 3 the cross sections calculated in the Born approximation with the same renormalization scale $(s/4)$ for the QCD α_S coupling and the b-quark pole mass $\overline{m}_b$ taken at the same scale $\overline{m}_b(\overline{m}_b)$ (upper curve). In addition, we plot the Born result for a b-quark mass taken at the scale $\sqrt{s}/2$ (lower curve); this shows that a large part of the one-loop suppression of the cross section comes from the running of the b-quark mass. However, note that for large angle scattering we observe a stronger suppression of the cross section due to other radiative corrections.

In Fig. 4 we show the scale dependence of the ratio $\sigma^{(0)+(1)}/\sigma^{(0)}$ of the whole one-loop cross section, integrated over the region $60° < \theta < 120°$ (that is, $|\cos\theta| < 1/2$), to that calculated in Born approximation with the pole mass $\overline{m}_b(\overline{m}_b)$ of the b-quark. The result is shown for two different masses of the $b\bar{b}$ system, namely $M_{bb} = \sqrt{s} = 120$ and

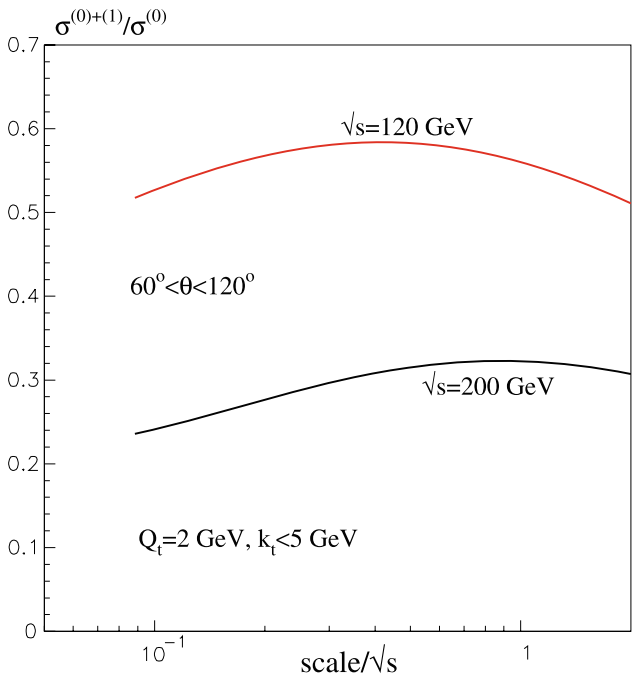

Fig. 4 The scale dependence of the ratio of the NLO exclusive $b\bar{b}$ cross section to that calculated in Born approximation

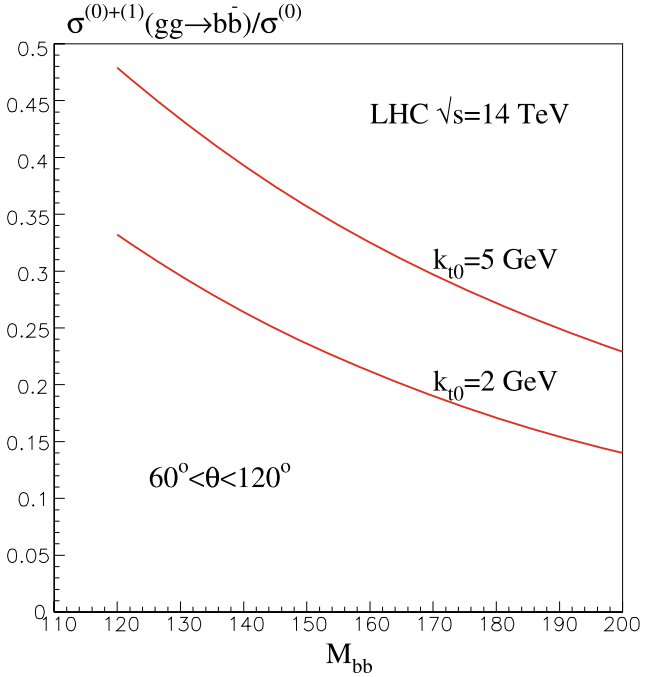

Fig. 5 The mass dependence of the ratio of the NLO exclusive $b\bar{b}$ cross section to that calculated in Born approximation

200 GeV. Here we put $Q_t = 2$ GeV and $k_{t0} = 5$ GeV. It is seen that the scale dependence in the region of $4\pi\mu^2 \sim s/4$ is rather flat.

Finally, in Fig. 5, we present the analogous ratio, $\sigma^{(0)+(1)}/\sigma^{(0)}$, of the CED cross sections, integrated over the region of $|\cos\theta| < 1/2$. this is the region expected at the LHC for exclusive $b\bar{b}$ production in the central region (with the rapidity of the $b\bar{b}$ pair $y = 0$). In this case the $gg^{\rm PP} \to b\bar{b}$ amplitudes $T_1^{\rm Born}$ and T_1, which enter the cross section (26), were convoluted with the luminosity amplitude (the integrand of (16)) following the Q_t-factorization prescription; that is, the amplitude $T_1(Q_t)$ was included inside the Q_t integral in (16). Again we show the results for two values of the infrared cut-off in the b jet definition—$k_{t0} = 5$ GeV and $k_{t0} = 2$ GeV—as a function of the mass M_{bb} of the $b\bar{b}$ pair for a scale equal to $M_{bb}/2$. Of course, for the smaller value, $k_{t0} = 2$ GeV, we have a stronger suppression, but this does not mean that by selecting narrower b jets (with a smaller cone size ΔR or a smaller k_{t0}) we can improve the Higgs signal-to-background ratio. The signal is diminished in the same way as the background when we suppress the emission of an additional gluon in the $H \to b\bar{b}$ decay; the exclusive $b\bar{b}$ cross section and the $H \to b\bar{b}$ signal have the same Sudakov suppression. Thus, in order not to lose statistics, it is better not to take the value of k_{t0} too small. On the other hand, k_{t0} should not be too large. Otherwise, we will not sufficiently suppress the three-particle, $gg^{\rm PP} \to b\bar{b} + g$, background [16]. From this viewpoint the predictions corresponding to $k_{t0} = 5$ GeV look appropriate.

In conclusion, the good news is that the radiative QCD (one-loop) corrections *suppress the exclusive $b\bar{b}$ background* (by a factor of about 2, or more for larger $b\bar{b}$-masses) for central exclusive diffractive (CED) Higgs production, in comparison with that calculated using the Born $gg^{\rm PP} \to b\bar{b}$ amplitude. As discussed in [3, 14], $b\bar{b}$ production in the $|J_z| = 2$ state is another background, which cannot be distinguished from the $H \to b\bar{b}$ decay. However, this contribution can be suppressed by selecting events with smaller transverse momenta of the forward outgoing protons [14]. Therefore, the exclusive gluon–gluon dijet production becomes the most important background for the CED Higgs process; see [3, 8] for a detailed discussion. In order to further suppress this QCD background we need a better experimental discrimination between b-quark and gluon jets; that is, to achieve a lower probability $P_{g/b}$ for misidentifying a gluon as a b jet.

Acknowledgements We thank Nigel Glover, Kemal Ozeren, Sven Moch, James Stirling, Robert Thorne, and especially Adrian Signer, for useful discussions. MGR thanks the IPPP at the University of Durham for hospitality, and VAK is grateful to the Kavli Institute for Theoretical Physics for hospitality during the completion of this work. The work was supported by INTAS grant 05-103-7515, by grant RFBR 07-02-00023 and by the Russian State grant RSGSS-5788.2006.02.

Appendix A: Master integrals

We present below the scalar master integrals needed to compute the one-loop effects shown in Fig. 2. The results contain the functions

$$F(\xi) \equiv \int_0^\xi {\rm d}x \frac{\ln(1+x)}{x} = -{\rm Li}_2(-\xi),$$

$$\rho \equiv \sqrt{s\big(s-4m^2\big)},$$

$$C_\epsilon \equiv -\frac{1}{\epsilon} - \ln\frac{m^2}{4\pi\mu^2},$$

where we work in $D = 4 + 2\epsilon$ dimensions.

Extra gluon between quark lines

Here, we give the integrals for diagrams 1–4 of Fig. 2, which involve the virtualities

$$a \equiv k^2 - m^2, \qquad b \equiv (k - p_{\rm B})^2 - m^2,$$

$$c \equiv (k + p_{\rm A} - p_1)^2 - m_g^2, \qquad d \equiv (k + p_{\rm A})^2 - m^2;$$

$$I^q_{0000}(s,t) \equiv \int \frac{{\rm d}^4k}{{\rm i}\pi^2}\frac{1}{abcd}$$

$$= \frac{1}{m^2 - t}\frac{1}{\rho}2\left[\ln\frac{\rho - s}{\rho + s}\right.$$

$$\times\left(\ln\left(1-\frac{t}{m^2}\right)-\frac{1}{2}\ln\frac{m_g^2}{m^2}\right)$$
$$+F\left(\frac{s}{\rho}\right)-F\left(-\frac{s}{\rho}\right)\Bigg],$$

$$I^q_{0001}(t)\equiv\int\frac{\mathrm{d}^4k}{\mathrm{i}\pi^2}\frac{1}{abc}=\frac{1}{m^2-t}\left[F\left(-\frac{t}{m^2}\right)+\frac{\pi^2}{6}\right],$$

$$I^q_{0010}(s)\equiv\int\frac{\mathrm{d}^4k}{\mathrm{i}\pi^2}\frac{1}{abd}=\frac{1}{2s}\ln^2\left(-\frac{s+\rho}{s-\rho}\right)-2F\left(-\frac{\rho+s}{2\rho}\right)$$
$$-F\left(-\frac{s+\rho}{s-\rho}\right)+F\left(-\frac{\rho-s}{s+\rho}\right),$$

$$I^q_{1010}(s)+C_\epsilon\equiv\int\frac{\mathrm{d}^4k}{\mathrm{i}\pi^2}\frac{1}{bd}=\left[\frac{\rho}{s}\ln\left(-\frac{s-\rho}{s+\rho}\right)+2\right]+C_\epsilon,$$

$$I^q_{0101}(t)+C_\epsilon\equiv\int\frac{\mathrm{d}^4k}{\mathrm{i}\pi^2}\frac{1}{ac}$$
$$=\left[2-\left(1-\frac{m^2}{t}\right)\ln\left(1-\frac{t}{m^2}\right)\right]+C_\epsilon,$$

$$\int\frac{\mathrm{d}^4k}{\mathrm{i}\pi^2}\frac{1}{cd}=\int\frac{\mathrm{d}^4k}{\mathrm{i}\pi^2}\frac{1}{bc}=C_\epsilon+2,$$

$$\int\frac{\mathrm{d}^4k}{\mathrm{i}\pi^2}\frac{1}{ad}=\int\frac{\mathrm{d}^4k}{\mathrm{i}\pi^2}\frac{1}{ab}=C_\epsilon.$$

Extra gluon coupling to gluons

Here, we give the integrals for diagrams 5 and 6 of Fig. 2, which involve the virtualities

$$a'\equiv k^2-m_g^2,\qquad b'\equiv(k-p_\mathrm{B})^2-m_g^2,$$
$$c'\equiv(k+p_\mathrm{A}-p_1)^2-m^2,\qquad d'\equiv(k+p_\mathrm{A})^2-m_g^2;$$

$$I^g_{0000}(s,t)\equiv\int\frac{\mathrm{d}^4k}{\mathrm{i}\pi^2}\frac{1}{a'b'c'd'}$$
$$=-\frac{1}{s}\frac{1}{m^2-t}\left[2\ln\frac{-s}{m_g^2}\ln\frac{m^2-t}{mm_g}-\frac{\pi^2}{2}\right],$$

$$I^g_{1000}(s)\equiv\int\frac{\mathrm{d}^4k}{\mathrm{i}\pi^2}\frac{1}{b'c'd'}$$
$$=\frac{1}{\rho}\Bigg[\ln\frac{-s}{m^2}\ln\left(-\frac{s+\rho}{s-\rho}\right)+\frac{1}{2}\ln^2\left(-\frac{s+\rho}{s-\rho}\right)$$
$$+\ln^2\left(-\frac{2s}{\rho-s}\right)-2F\left(-\frac{s+\rho}{s-\rho}\right)$$
$$-2F\left(-\frac{s+\rho}{2s}\right)-2F\left(\frac{2s}{\rho-s}\right)-\pi^2\Bigg],$$

$$I^g_{0100}(t)\equiv\int\frac{\mathrm{d}^4k}{\mathrm{i}\pi^2}\frac{1}{a'c'd'}$$
$$=\frac{1}{t-m^2}\left[F\left(\frac{t}{m^2-t}\right)+\frac{1}{2}\ln^2\left(\frac{m^2-t}{m^2}\right)\right.$$
$$\left.-\ln\frac{m_g^2}{m^2}\ln\left(\frac{m^2-t}{m^2}\right)+\frac{1}{4}\ln^2\frac{m_g^2}{m^2}+\frac{\pi^2}{12}\right],$$

$$I^g_{1010}(s)+C_\epsilon\equiv\int\frac{\mathrm{d}^4k}{\mathrm{i}\pi^2}\frac{1}{b'd'}=\left[2+\ln\frac{m^2}{-s}\right]+C_\epsilon,$$

$$I^g_{0101}(t)+C_\epsilon\equiv\int\frac{\mathrm{d}^4k}{\mathrm{i}\pi^2}\frac{1}{a'c'}$$
$$=\left[2-\left(1-\frac{m^2}{t}\right)\ln\left(1-\frac{t}{m^2}\right)\right]+C_\epsilon,$$

$$\int\frac{\mathrm{d}^4k}{\mathrm{i}\pi^2}\frac{1}{c'd'}=\int\frac{\mathrm{d}^4k}{\mathrm{i}\pi^2}\frac{1}{b'c'}=C_\epsilon+2,$$

$$\int\frac{\mathrm{d}^4k}{\mathrm{i}\pi^2}\frac{1}{a'd'}=C_\epsilon+\ln\frac{m^2}{m_g^2}.$$

Extra gluon between a quark and a gluon line

Here, we give the integrals for diagrams 7–10 of Fig. 2, which involve the virtualities

$$\tilde a\equiv k^2-m_g^2,\qquad \tilde b\equiv(k+p_\mathrm{B})^2-m_g^2,$$
$$\tilde c\equiv(k+p_1-p_\mathrm{A})^2-m^2,\qquad \tilde d\equiv(k+p_1)^2-m^2,$$
$$\tilde e\equiv(k-p_\mathrm{A})^2-m_g^2,\qquad \tilde f\equiv(k-p_2)^2-m^2;$$

$$I^{qg}_{0000}(u,t)=\int\frac{\mathrm{d}^4k}{\mathrm{i}\pi^2}\frac{1}{\tilde a\tilde b\tilde c\tilde d}$$
$$=\frac{1}{m^2-u}\frac{1}{m^2-t}2\left[\ln\frac{m^2-u}{mm_g}\ln\frac{m^2-t}{mm_g}+\frac{\pi^2}{12}\right],$$

$$I^{qg}_{1000}(u)=\int\frac{\mathrm{d}^4k}{\mathrm{i}\pi^2}\frac{1}{\tilde b\tilde c\tilde d}=\frac{1}{u-m^2}\left[F\left(-\frac{u}{m^2}\right)+\frac{\pi^2}{6}\right],$$

$$I^{qg}_{0010}(u)=\int\frac{\mathrm{d}^4k}{\mathrm{i}\pi^2}\frac{1}{\tilde a\tilde e\tilde f}$$
$$=\frac{1}{u-m^2}\left[F\left(\frac{u}{m^2-u}\right)+\frac{1}{2}\ln^2\frac{m^2-u}{m_g^2}\right.$$
$$\left.-\frac{1}{4}\ln^2\frac{m^2}{m_g^2}+\frac{\pi^2}{12}\right],$$

$$I^{qg}_{1010}(u)+C_\epsilon=\int\frac{\mathrm{d}^4k}{\mathrm{i}\pi^2}\frac{1}{\tilde e\tilde f}$$
$$=\left[2-\left(1-\frac{m^2}{u}\right)\ln\left(1-\frac{u}{m^2}\right)\right]+C_\epsilon,$$

$$\int\frac{\mathrm{d}^4k}{\mathrm{i}\pi^2}\frac{1}{\tilde c\tilde f}=C_\epsilon,\qquad\int\frac{\mathrm{d}^4k}{\mathrm{i}\pi^2}\frac{1}{\tilde a\tilde e}=C_\epsilon+\ln\frac{m^2}{m_g^2},$$

$$\int\frac{\mathrm{d}^4k}{\mathrm{i}\pi^2}\frac{1}{\tilde c\tilde e}=\int\frac{\mathrm{d}^4k}{\mathrm{i}\pi^2}\frac{1}{\tilde a\tilde f}=C_\epsilon+2.$$

Appendix B: $\overline{\text{MS}}$ renormalization

It is useful to recall the well known one-loop renormalization in the $\overline{\text{MS}}$ scheme. The bare quark mass m_0 and coupling constant α_0 are expressed through their renormalized values m and α_S in the renormalized amplitude T^R. In addition, the renormalization of the quark and gluon wavefunctions has to be taken into account, which results in factors Z_2 and Z_3. The relation between the bare and physical coupling at one-loop order reads

$$\alpha_0 = \alpha\left[1+\frac{1}{\epsilon}\beta_0\alpha+\mathcal{O}\left(\alpha^2\right)\right] \equiv \alpha + \alpha_0^{(1)}(\alpha),$$

$$\beta_0 = \frac{11}{3}N_c - \frac{2}{3}n_f.$$

Similarly

$$Z_{2,3} = 1 + Z_{2,3}^{(1)},$$

where $Z_{2,3}^{(1)}$ are given by the first-order corrections to the quark and gluon propagators. The correction to the bare quark mass,

$$m_0(m) = m + m_0^{(1)}(m) = m + \Sigma(m),$$

is determined by the first-order quark self-energy $\Sigma(\not{p})$. With these factors included, the first-order amplitude takes the form

$$T^R = T^{\text{one-loop}}(\alpha_0, m_0) + \left[Z_2^{(1)} + Z_3^{(1)} + m_0^{(1)}(m) + \alpha_0^{(1)}(\alpha)\right]T^{\text{Born}}.$$

The quark one-loop self-energy reads

$$\Sigma(\hat{p}) = -\frac{\alpha_S}{4\pi}\Gamma\left(2-\frac{D}{2}\right)\int_0^1 \mathrm{d}x\left[Dm + \overline{x}(2-D)\not{p}\right] \times \left(\frac{-x\overline{x}p^2 + xm^2 + \overline{x}m_g^2}{4\pi\mu^2 e^{\gamma}}\right)^{\frac{D}{2}-2},$$

where $\overline{x} \equiv 1-x$ and γ is the Euler constant. As a result

$$\Sigma(m) = -\frac{\alpha_S}{4\pi}mC_F(3C_\epsilon + 4) + \mathcal{O}(\epsilon),$$

$$Z_2^{(1)} = -\left.\frac{\partial\Sigma}{\partial p}\right|_{p=m} = -\frac{\alpha_S}{4\pi}C_F\left(C_\epsilon + 4 - 2\ln\frac{m^2}{m_g^2}\right) + \mathcal{O}(\epsilon).$$

The gluon polarization operator in Feynman gauge,

$$\Pi^{\mu\nu}(p) = \left(g^{\mu\nu}p^2 - p^\mu p^\nu\right)\pi\left(p^2\right),$$

reads to one-loop order

$$\pi(p^2) = \frac{\alpha_S}{4\pi}\frac{\Gamma^2(\frac{D}{2}-1)}{\Gamma(D-2)}\Gamma\left(2-\frac{D}{2}\right)\left(-\frac{p^2}{4\pi\mu^2e^{\gamma}}\right)^{\frac{D}{2}-2} \times\left[N_c\frac{3D-2}{2(D-1)} - n_f\frac{(D-2)}{D-1}\right].$$

With $D = 4+2\epsilon$, one gets

$$Z_3^{(1)} = \pi\left(p^2\right) = \frac{\alpha_S}{4\pi}\left[N_c\left(\frac{5}{3}C_\epsilon + \frac{5}{3}\ln\frac{m^2}{-p^2} + \frac{31}{9}\right) - \frac{1}{2}n_f\left(\frac{4}{3}C_\epsilon + \frac{4}{3}\ln\frac{m^2}{-p^2} + \frac{20}{9}\right) + \mathcal{O}(\epsilon)\right].$$

References

1. V.A. Khoze, A.D. Martin, M.G. Ryskin, Eur. Phys. J. C **14**, 525 (2000)
2. V.A. Khoze, A.D. Martin, M.G. Ryskin, Eur. Phys. J. C **23**, 311 (2002)
3. A. De Roeck, V.A. Khoze, A.D. Martin, R. Orava, M.G. Ryskin, Eur. Phys. J. C **25**, 391 (2002)
4. J.R. Forshaw, PoS **DIFF2006**, 055 (2006). arXiv:hep-ph/0611274
5. V.A. Khoze, M.G. Ryskin, A.D. Martin, in *Hamburg 2007, Blois07, Forward Physics and QCD*, p. 452. arXiv:0705.2314 [hep-ph]
6. C. Royon, arXiv:0805.0261 [hep-ph]
7. A.B. Kaidalov, V.A. Khoze, A.D. Martin, M.G. Ryskin, Eur. Phys. J. C **33**, 261 (2004)
8. S. Heinemeyer et al., Eur. Phys. J. C **53**, 231 (2008)
9. B. Cox, F. Loebinger, A. Pilkington, J. High Energy Phys. **0710**, 090 (2007)
10. J.R. Forshaw, J.F. Gunion, L. Hodgkinson, A. Papaefstathiou, A.D. Pilkington, arXiv:0712.3510 [hep-ph]
11. M. Albrow et al., CERN-LHCC-2005-025. arXiv:0806.0302 [hep-ex]
12. B.E. Cox, arXiv:hep-ph/0609209
13. V.A. Khoze, A.D. Martin, M.G. Ryskin, in *Proc. of 8th Int. Workshop on Deep Inelastic Scattering and QCD (DIS2000), Liverpool*, ed. by J. Gracey, T. Greenshaw (World Scientific, Singapore, 2001), p. 592. arXiv:hep-ph/0006005
14. V.A. Khoze, A.D. Martin, M.G. Ryskin, Eur. Phys. J. C **19**, 477 (2001). Eur. Phys. J. C **20**, 599 (2001) (Erratum)
15. V.S. Fadin, V.A. Khoze, A.D. Martin, Phys. Rev. D **56**, 484 (1997)
16. V.A. Khoze, M.G. Ryskin, W.J. Stirling, Eur. Phys. J. C **48**, 477 (2006). arXiv:hep-ph/0607134
17. D.L. Borden, V.A. Khoze, W.J. Stirling, J. Ohnemus, Phys. Rev. D **50**, 4499 (1994)
18. S.J. Parke, T.R. Taylor, Phys. Rev. Lett. **56**, 2459 (1986).
19. F.A. Berends, W.T. Giele, Nucl. Phys. B **306**, 759 (1988)
20. M.L. Mangano, S.J. Parke, Phys. Rep. **200**, 301 (1991)
21. V.A. Khoze, A.D. Martin, M.G. Ryskin, Phys. Lett. B **650**, 41 (2007)
22. W.A. Bardeen, A.J. Buras, D.W. Duke, T. Muta, Phys. Rev. D **18**, 3998 (1978)
23. G. Jikia, A. Tkabladze, Phys. Rev. D **54**, 2030 (1996)
24. M. Melles, W.J. Stirling, Phys. Rev. D **59**, 094009 (1999)

25. M. Melles, W.J. Stirling, Eur. Phys. J. C **9**, 101 (1999)
26. M. Melles, W.J. Stirling, Nucl. Phys. B **564**, 325 (2000)
27. M. Melles, W.J. Stirling, V.A. Khoze, Phys. Rev. D **61**, 054015 (2000)
28. V.V. Sudakov, Sov. Phys. JETP **3**, 65 (1956)
29. V.A. Khoze, A.D. Martin, M.G. Ryskin, Eur. Phys. J. C **18**, 167 (2000)
30. M.G. Ryskin, A.D. Martin, V.A. Khoze, Eur. Phys. J. C **54**, 199 (2008)
31. E.A. Kuraev, L.N. Lipatov, V.S. Fadin, Phys. Lett. B **60**, 50 (1975)
32. I.I. Balitsky, L.N. Lipatov, V.S. Fadin, in *Proceedings, Physics of Elementary Particles*, Leningrad, 1979, p. 109
33. Z. Kunszt, A. Signer, Z. Trocsanyi, Nucl. Phys. B **411**, 397 (1994)
34. Z. Kunszt, A. Signer, Z. Trocsanyi, Nucl. Phys. B **605**, 486 (2001)
35. C. Anastasiou, E.W.N. Glover, M.E. Tejeda-Yeomans, Nucl. Phys. B **629**, 255 (2002)
36. M.A. Kimber, A.D. Martin, M.G. Ryskin, Phys. Rev. D **63**, 144027 (2001)
37. A.D. Martin, M.G. Ryskin, Phys. Rev. D **64**, 094017 (2001)